Worked-out problems, PiTP 2011, group 22

Michela D'Onofrio, Soichiro Isoyama,
Austin Joyce, Ted van der Aalst

July 28, 2011

1.4 Action for AdS_4

As the AdS metric is

$$ds^2 = d\rho^2 + \sinh^2\rho\, d\Omega_3^2\,, \tag{1}$$

the extrinsic curvature $K = \frac{1}{2}h^{ab}\partial_n h_{ab}$, with h_{ab} the boundary metric and ∂_n the derivative in the normal direction, is

$$K = \frac{1}{2}\mathrm{Tr}\left[\begin{pmatrix}1 & 0\\ 0 & \sinh^2\rho\,\Omega_3\end{pmatrix}^{-1}\begin{pmatrix}0 & 0\\ 0 & 2\sinh\rho\,\cosh\rho\,\Omega_3\end{pmatrix}\right] = 3\coth\rho\,, \tag{2}$$

where Ω_3 denotes the metric on S^3. Integrating over the sphere S^3 after regulating with a cutoff ρ_c, one finds

$$\int_{\partial\Sigma_4} K = 3\coth\rho_c\,\mathrm{Vol}(S^3)\,. \tag{3}$$

Since in AdS, the Ricci scalar is a constant, the other integral in the on shell action is simply proportional to

$$\begin{aligned}\frac{1}{\mathrm{Vol}(S^3)}\int_{\Sigma_4}\sqrt{g} &= \int_0^{\rho_c}\sinh^3\rho = \int_0^{\rho_c}\left(\sinh\rho\,\cosh^2\rho\,-\sinh\rho\right)\\ &= \cosh\rho\,(\frac{1}{3}\cosh^2\rho\,-1)\Big|_0^{\rho_c} = \frac{2}{3}+\cosh\rho_c\,(\frac{1}{3}\cosh^2\rho_c\,-1)\,.\end{aligned} \tag{4}$$

Combining these two results,

$$\begin{aligned}&\Psi = Z \sim e^{-S_E} =\\ &\exp\left\{\frac{R_{AdS}^2}{16\pi G_N}\mathrm{Vol}(S^3)\left[(R+6)\left(\frac{2}{3}+\cosh\rho_c\,(\frac{1}{3}\cosh^2\rho_c\,-1)\right)-6\coth\rho_c\right]\right\}\,.\end{aligned} \tag{5}$$

Discarding the divergent terms as $\rho_c\to\infty$ the only finite contribution is

$$\Psi = Z \sim e^{-S_E} = \exp\left\{\frac{R_{AdS}^2}{24\pi G_N}\mathrm{Vol}(S^3)(R+6)\right\}\,. \tag{6}$$

1.5 Action for dS_4

We can follow the same steps as in exercise 1.4. The extrinsic curvature now is

$$K = 3\tanh\tau \ , \tag{7}$$

while the first term in the Hartle-Hawking analytic continuation of S_E is proportional to

$$\begin{aligned}\frac{1}{\mathrm{Vol}(S^3)}\int_{\Sigma_4}\sqrt{g} &= \int_0^{\rho_c}\sinh^3\tau \\ &= \sinh\tau\,(\frac{1}{3}\sinh^2\tau\ +1)\Big|_0^{\tau_c} = 0+\sinh\tau_c\,(\frac{1}{3}\sinh^2\tau_c\ +1)\,.\end{aligned} \tag{8}$$

Because $\lim_{\tau_c\to\infty}\tanh\tau_c = 1$, we see that in this case the boundary term is not infinite. In fact it is the only finite contribution as $\tau_c\to\infty$,

$$\begin{aligned}\Psi = Z \sim e^{iS} = \\ &\exp\left\{i\frac{R_{dS}^2}{16\pi G_N}\mathrm{Vol}(S^3)\left[(R+6)\sinh\tau_c\,(\frac{1}{3}\sinh^2\tau_c\ +1)+6\right]\right\} \\ &= infinity\times\exp\left\{i\frac{3R_{dS}^2}{8\pi G_N}\mathrm{Vol}(S^3)\right\}\ .\end{aligned} \tag{9}$$

Compared to the AdS-case, the finite contribution is coming from another part of the on shell action. Plugging in the value for the Ricci scalar of AdS, $R=-12$, the results for the dS and AdS cases match almost, but not quite.

2.2 n–point function in de Sitter

We know that de Sitter space has a scaling symmetry

$$\begin{aligned}x &\longrightarrow \lambda x \\ k &\longrightarrow \frac{k}{\lambda}\ .\end{aligned} \tag{10}$$

From this, as noted in the lectures, we may deduce that the curvature perturbation, ζ_k, scales as

$$\zeta_k \longrightarrow \lambda^3\zeta_{\lambda k}\ . \tag{11}$$

Let's convince ourselves that this is true. We may write the field $\zeta(x)$ in Fourier space as

$$\zeta(x) = \int \mathrm{d}^3k e^{i\vec{k}\cdot\vec{x}}\zeta_k\ . \tag{12}$$

Under the rescaling (10), the real space field is invariant

$$\zeta(x)\longrightarrow\zeta(\lambda x) = \int\frac{\mathrm{d}^3k}{\lambda^3}e^{i\frac{\vec{k}}{\lambda}\cdot\lambda\vec{x}}\widetilde{\zeta}_{k/\lambda} = \zeta(x) \tag{13}$$

from which we deduce that $\widetilde{\zeta_k} = \lambda^3 \zeta_{\lambda k}$. Now, consider an n–point function $\langle \zeta_{k_1} \zeta_{k_2} \dots \zeta_{k_n} \rangle$, we know that the n–point function must be homogeneous in k, so we may write it schematically

$$\langle \zeta_{k_1} \zeta_{k_2} \dots \zeta_{k_n} \rangle \sim \delta \left(\sum \vec{k} \right) F \left(k^{\mathrm{A}} \right) \tag{14}$$

We know that the left hand side scales by a factor of λ^{3n} while the right hand side scales by a factor of $\lambda^{3-\mathrm{A}}$, because the delta function scales by λ^3, from which we deduce that the n point amplitude must be a homogeneous function of k to the $-3(n-1)$

$$\langle \zeta_{k_1} \zeta_{k_2} \dots \zeta_{k_n} \rangle \sim \delta \left(\sum \vec{k} \right) F \left(k^{-3(n-1)} \right) \ . \tag{15}$$

3.5 Transition matrix with terminal vacuum

Because 0 is a terminal vacuum, $\gamma_{1,0} = \gamma_{2,0} = 0$, i.e. the decay rate from 0 to either 1 or 2 is 0. In such a situation, the transition matrix, $\delta P_a = P_a(n+1) - P_a(n) = -\sum_b \gamma_{b,a} P_a(n) + \sum_b \gamma_{a,b} P_b(n)$, reduces to

$$M = \begin{pmatrix} 0 & \gamma_{0,1} & \gamma_{0,2} \\ 0 & -\gamma_{0,1} - \gamma_{2,1} & \gamma_{1,2} \\ 0 & \gamma_{2,1} & -\gamma_{0,2} - \gamma_{1,2} \end{pmatrix} \ , \tag{16}$$

whose characteristic polynomial equals

$$0 = -\lambda \left(\lambda^2 - \lambda \mathrm{Tr} A + \det A \right) \ , \tag{17}$$

which obviously shows there is a zero eigenvalue (with eigenvector $(1,0,0)$). The matrix A is the lower right 2×2 matrix of M and it is straightforward to check that $\mathrm{Tr} A < 0$, while $\det A > 0$. By writing out $\mathrm{Tr}^2 A - 4 \det A$ in terms of the γ's one can verify explicitly that the discriminant is positive. As a result, both solutions

$$\lambda_\pm = \frac{1}{2} \mathrm{Tr} A \pm \frac{1}{2} \sqrt{\mathrm{Tr}^2 A - 4 \det A} \ , \tag{18}$$

of the quadratic equation in (17) are real and negative.

To find out how the probability to be in vacuum a changes over time, we simply have to solve the differential equation

$$\dot{P}_a(t) = M_{ab} P_b(t) \ , \tag{19}$$

which has as a solution

$$P_a(t) = S \begin{pmatrix} 1 & 0 & 0 \\ 0 & e^{\lambda_+ t} & 0 \\ 0 & 0 & e^{\lambda_- t} \end{pmatrix} S^{-1} P_a(0) \ . \tag{20}$$

The matrix S is the matrix consisting of the eigenvectors of M and will consist simply of coefficients depending on the γ's. Hence $P_1(t)$ and $P_2(t)$ are given by

$$P_{1,2}(t) = a_{1,2}e^{\lambda_+ t} + b_{1,2}e^{\lambda_- t} \ , \tag{21}$$

with a_1, a_2, b_1, b_2 some constants. Both $P_1(t)$ and $P_2(t)$ are monotonically decreasing functions for $\lambda_\pm < 0$.

Nevertheless the number of vacua a at a time t in a universe expanding at a rate e^r, is given by

$$N_a(t) = P_a(t)r^t = P_a(t)e^{rt} \ . \tag{22}$$

Therefore, assuming the elements of the transition matrix to be small, i.e. $r > |\lambda_\pm|$, the number of vacua 1 and 2 increases with time.

4.2 Various aspects of string inflationary models

a) Consider gravity in D dimensions with $D-4$ of its dimensions compactified on a manifold X. For simplicity we will take this space to be a flat torus. Our starting point is the D dimensional Einstein action

$$S = \int \mathrm{d}^D x \sqrt{-g^{(D)}}\mathcal{R}^{(D)} \ , \tag{23}$$

where $M^2_{(D)}$ is the D dimensional Planck mass. For simplicity, we assume a product manifold structure $\mathcal{M} \times \mathbb{T}^{D-4}$, with line element

$$ds^2 = g_{\mu\nu}dx^\mu \otimes dx^\nu + V_X^2(x)h_{AB}dy^A \otimes dy^B \tag{24}$$

where $g_{\mu\nu}$ are the components of the 4 dimensional metric, and h_{AB} is the metric on the internal space X. Integrating over the internal dimensions, we will obtain the volume factor $V_X(x)$. We also note that

$$\mathcal{R}^{(D)} = \mathcal{R}^{(4)} + (D-4)(D-5)g^{\mu\nu}\partial_\mu \log V_X(x)\partial_\nu \log V_X(x) \ , \tag{25}$$

Then, we have after integrating out the internal space

$$S = \int \mathrm{d}^4 x \sqrt{-g^{(4)}}V_X^{D-4}(x)\left[\mathcal{R}^{(4)} + (D-4)(D-5)g^{\mu\nu}\partial_\mu \log V_X(x)\partial_\nu \log V_X(x)\right] \tag{26}$$

We perform a conformal transformation to go to Einstein frame

$$g^E_{\mu\nu} = V_X^{D-4}(x)g_{\mu\nu} \ , \tag{27}$$

which leads to the action

$$S = \int \mathrm{d}^4 x \sqrt{-g_E^{(4)}}\left(\mathcal{R}_E^{(4)} - \frac{1}{2}(D-4)(D-2)g_E^{\mu\nu}\partial_\mu \log V_X(x)\partial_\nu \log V_X(x)\right) \ . \tag{28}$$

If we now canonically normalize the field, we have

$$\sqrt{(D-4)(D-2)}\log V_X(x) \equiv \frac{1}{c_X}\log V_X(x) = \sigma \tag{29}$$

so

$$V_X(x) = e^{c_X\sigma} \ . \tag{30}$$

b) Orientifolds are not dynamical objects. They don't have microphysical degrees of freedom like D–branes, which have open strings ending on them. An orientifold plane is a geometrical object, like an orbifolding. As a result, the normal reasoning why negative mass modes provide problems, e.g. they can be used to lower the entropy of a black hole or they can be used to pair produce an infinite nunmber of particles, or in general any problems that arise when the null energy condition is violated, do not apply to orientifolds. They are static objects which do not allow for any (perturbative) fluctuations.

c) We want to find the gauge transformation for C_p needed to make the object

$$|\mathrm{d}C_p + B \wedge \mathrm{d}C_{p-2}|^2 \ , \tag{31}$$

gauge invariant under $B \longrightarrow B + \mathrm{d}\Lambda_1$. Consider the object $\mathrm{d}C_p + B \wedge \mathrm{d}C_{p-2}$ and perform a gauge transformation

$$\mathrm{d}C_p + B \wedge \mathrm{d}C_{p-2} \longrightarrow \mathrm{d}C_p + B \wedge \mathrm{d}C_{p-2} + \mathrm{d}\Lambda_1 \wedge \mathrm{d}C_{p-2} + \mathrm{d}\Delta C_p \ . \tag{32}$$

In order for this to be invariant, we must have

$$\Delta C_p = -\Lambda_1 \wedge \mathrm{d}C_{p-2} \ . \tag{33}$$

Quickly plugging this in verifies this. There is another possible transformation rule we might have chosen. We could have taken $\Delta C_p = \mathrm{d}\Lambda_1 \wedge C_{p-2}$, but this just differs from (33) by pure gauge. Indeed,

$$\mathrm{d}\Lambda_1 \wedge \mathrm{d}C_{p-2} - \Lambda_1 \wedge \mathrm{d}C_{p-2} = \mathrm{d}\left(\Lambda_1 \wedge C_{p-2}\right) \tag{34}$$

is exact.

d) We follow the steps in the original paper by Baumann and McAllister, hep-th/0610285. The 10-dimensional spacetime with metric

$$h^{-1/2}(y) g^{(4)}_{\mu\nu} dx^\mu dx^\nu + h^{1/2}(y) g^{(6)}_{ij} dy^i dy^j \ , \tag{35}$$

may locally be viewed to be equivalent to $AdS_5 \times X_5$, where

$$g_{ij} dy^i dy^j = dr^2 + r^2 ds^2_{X_5} \tag{36}$$

and the warp factor $h(r)$ is given by $h(r) = R^4/r^4$. The internal space therefore has volume

$$V_6 = \int d^6y \sqrt{g} h = \mathrm{Vol}(X_5) \int_0^{r_{UV}} dr r^5 h(r) = \frac{1}{2}\mathrm{Vol}(X_5) R^4 r^2_{UV} \ , \tag{37}$$

where r_{UV} is the cutoff of the throat.

For the Einstein–Hilbert term in a compactification scenario, the four-dimensional Planck mass M_{pl} is given by

$$M_{pl}^2 = \frac{V_6}{\kappa_{10}^2} \,, \tag{38}$$

where $\kappa_{10}^2 = \frac{1}{2}(2\pi))7g_s^2(\alpha')^4$, since

$$S \sim \frac{1}{\kappa_{10}^2}\int \sqrt{-g^{(10)}}R^{(10)} \sim \frac{V_6}{\kappa_{10}^2}\int \sqrt{-g^{(4)}}R^{(4)} + \dots \,. \tag{39}$$

Combining both results and using the Lyth bound $r \lesssim \frac{8}{30^2}\frac{\Delta\phi^2}{M_{pl}^2}$, we find

$$r \lesssim \frac{8}{30^2}\frac{\Delta\phi^2\kappa_{10}^2}{\frac{1}{2}\mathrm{Vol}(X_5)R^4 r_{UV}^2} < \frac{4}{15^2}\frac{r_{UV}^2\kappa_{10}^2}{\alpha'^2\mathrm{Vol}(X_5)R^4 r_{UV}^2} = \frac{4}{15^2}\frac{\kappa_{10}^2}{\alpha'^2\mathrm{Vol}(X_5)R^4} \,. \tag{40}$$

5.5 Parameter dependence of the CMB

The plots

The diagrams shown are produced by using the online tool CAMB at lambda.gsfc.nasa.gov. Since the sum of $\Omega_\Lambda + \Omega_{CDM} + \Omega_b = 1$ we have chosen to vary each of the three contributions while keeping the respective ratio between the other two fixed. That is, while varying Ω_b we kept $\Omega_\Lambda/\Omega_{CDM}h^2 = 3$, for Ω_{CDM} we took $\Omega_\Lambda/\Omega_b h^2 = 15$ and for Ω_Λ we made sure that $\Omega_{CDM}/\Omega_b = 5$. In each of the plots, we have plotted the actual WMAP data, including error bars, and a family of ten lines with differing $\Omega_b h^2$, $\Omega_{CDM}h^2$ or Ω_Λ respectively.

Physical interpretation

Ω_b

The plot shows that with increasing Ω_b, the first peak grows while the second mode is damped out. The third mode is enhanced again.

This feature is expected as Ω_b is responsible for the moment of hydrostatic equilibrium. With increasing Ω_b, hydrostatic equilibrium will happen later. If one then squares the oscillations, the odd peaks will become higher while the even peaks are smoothened out.

This observation is consistent with Samtleben 2007 (Annu. Rev. Nucl. Part. Sci. 57:24583), who writes "As to Ω_b, increasing it decreases the second peak but enhances that of the third because the inertia in the photon-baryon fluid is increased, leading to hotter compressions and cooler rarefactions."

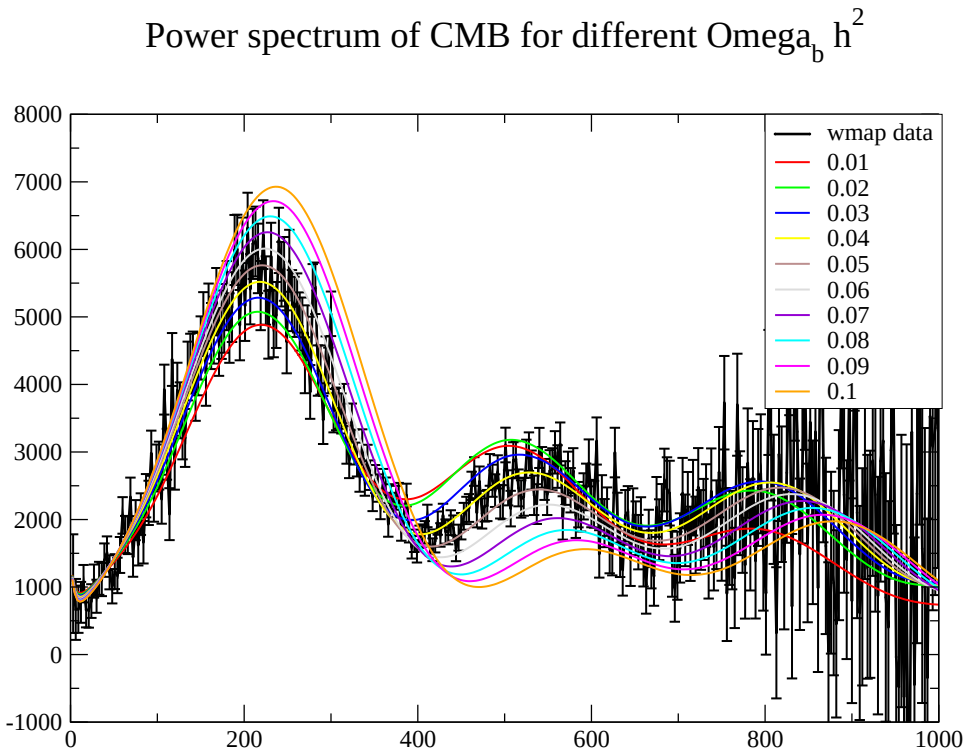

Ω_{CDM}

The plot shows that with increasing Ω_{CDM}, the relative size of the first peak to the other peaks is decreasing. Overall the size of the oscillations damp out with increasing Ω_{CDM}.

Again, these effects are expected as a change in Ω_{CDM} will change the moment of matter/radiation equality, which in general is responsible for a relative enhancement of the low vs. the high l-modes, as explained in the lectures by Matias Zaldarriaga.

In the words of Samtleben 2007, "Increasing Ω_{CDM} decreases the peak heights. With greater matter density, the era of equality is pushed to earlier redshifts, allowing the dark matter more time to form deeper potential wells. When the baryons fall into these wells, their mass has less effect on the development of the potential so that the escaping photons are less redshifted than they would be, yielding a smaller temperature contrast."

Ω_Λ

The dependence on Ω_Λ is more subtle. In our plot, the first peak is first decreasing with increasing Ω_Λ, but later increases. The other peaks are mostly flat, until $\Omega_\Lambda \gtrsim 0.6$, where the second peak becomes more apparent.

This behaviour is somewhat unexpected, because according to Takahiko Matsubara 2007

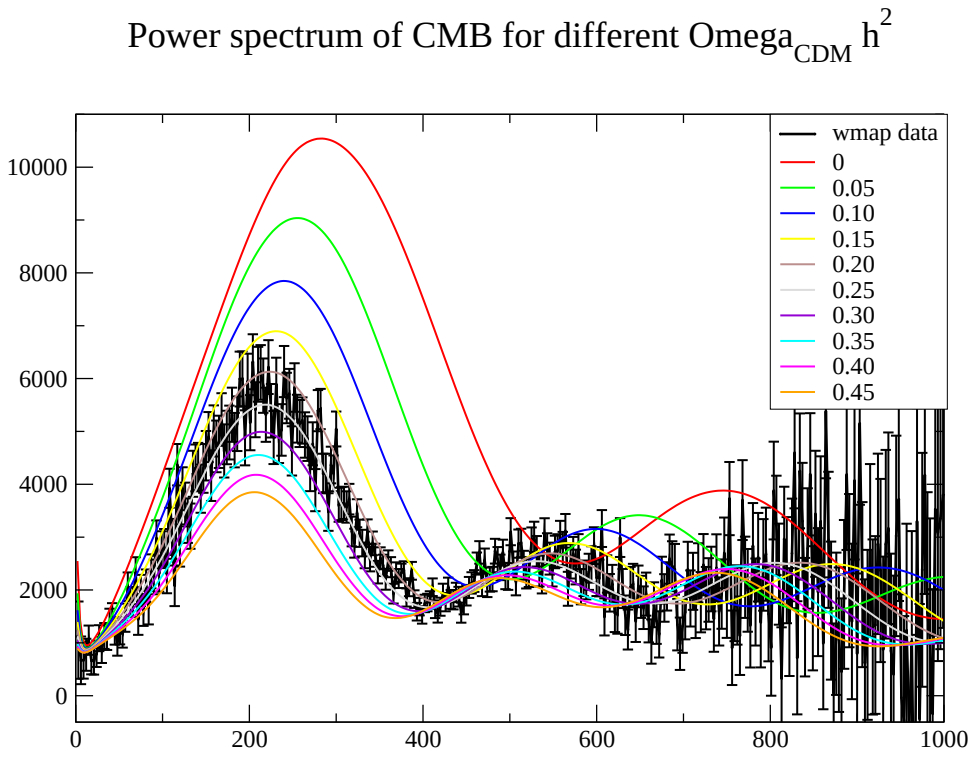

(Introduction to Modern Cosmology: Coevolution of Spacetime and Matter, University of Tokyo Press), a change in Ω_Λ should just produce a shift of the peaks in l-space.

Physically one can understand this by noting that the angular modes l are related to the k-modes through $l \sim kD$, where D is the distance to the last scattering surface. By changing Ω_Λ, the distance to the last scattering surface is also changed, which induces the shift of the power spectrum.

One can recognize another effect. The modes from the cosmological constant dominated era, i.e. the very small l-modes, are affected by the late-time integrated Sachs-Wolfe effect. As photons travel through spacetime, the gravitational potential wells evolve gradually, causing a redshift to the photons. As a result the oscillations we see in the power spectrum are enhanced for the very late-time modes, small l, that have just crossed the horizon. Increasing Ω_Λ should increase this enhancement, as the epoch of cosmological constant domination starts earlier. We do not really observe this feature in the plot.

Parameter range

Comparing our plots with the given error bars by the WMAP collaboration, we can make a rough estimate on the values for $\Omega_b h^2$, $\Omega_{CDM} h^2$ and Ω_Λ.

Considering the Ω_b-plot, we would estimate $\Omega_b h^2$ to be between 0.03 and 0.06. The value

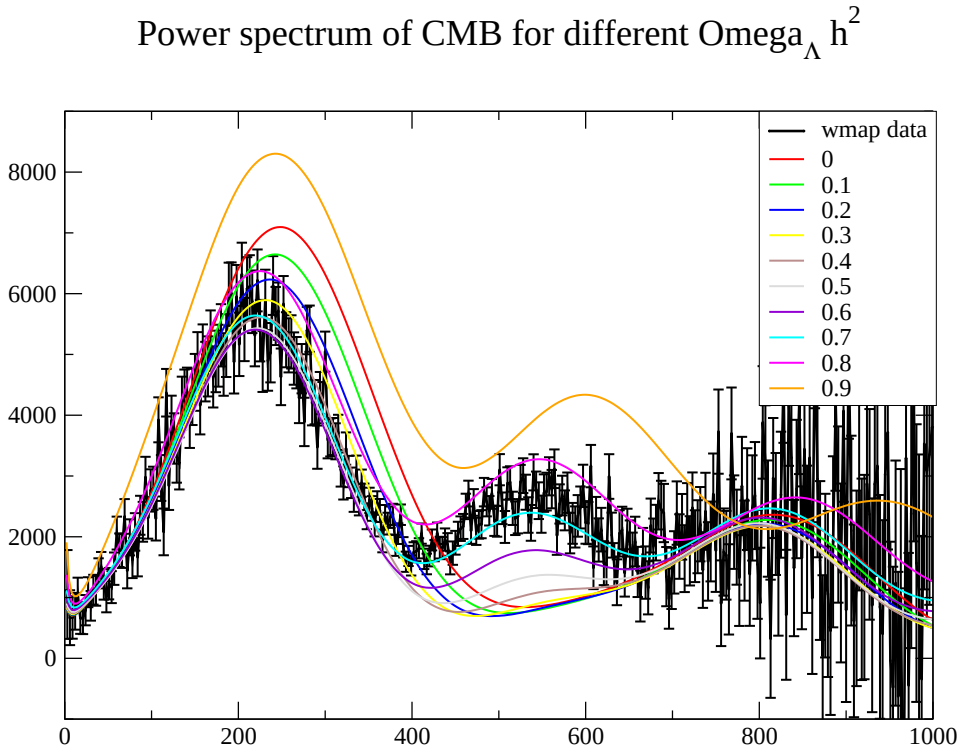

of WMAP7 is put at 0.02258 ± 0.00057. This is a rather uncomfortable situation, which possible is due to the non-realistic values we have taken for Ω_Λ and $\Omega_{CDM}h^2$.

Our estimate for $\Omega_{CDM}h^2$ is 0.2 to 0.3, compared to the 0.1109 ± 0.0056 of WMAP7. Again our estimate falls outside the region of the WMAP7-value. Our estimate for Ω_Λ is 0.7 to 0.8, which does match with WMAP7's estimate of 0.734 ± 0.029.

Unexpectedly it seems to matter much if one fits for all three values at once (as WMAP7 has done), or for each of the parameters individually. Another possibility is that it matters much which ratios one chooses while varying the other parameter.